2002-01-1626

In-Cylinder Penetration and Break-Up of Diesel Sprays Using a Common-Rail Injection System

D.A. Kennaird, C. Crua, J. Lacoste and M.R. Heikal
University of Brighton - UK

M.R. Gold, N.S. Jackson
Ricardo Consulting Engineers

ABSTRACT

As part of an ongoing investigation, the influence of in-cylinder charge density, and injector nozzle geometry on the behaviour of diesel sprays were examined using high-speed imaging. Both liquid and vapour penetration profiles were investigated in operating conditions representative of a modern turbocharged after-cooled HSDI diesel engine. These conditions were achieved in an optical rapid compression machine fitted with a common rail fuel injection system.

Differences in spray liquid and vapour penetrations were observed for different nozzle geometries and in-cylinder conditions over a range of injection fuelling representative of those in a typical engine map. Investigation into the differences in spray structure formed by multi-hole and single-hole injections were also undertaken. The results of the spray penetration profiles from the experiments were compared to empirical correlations in the literature and differences observed were attributed to flow structures within the nozzle, which are not taken into account by these correlations.

INTRODUCTION

The stringent emission legislation placed upon the modern diesel engine poses a challenge to engine designers. In order to meet these standards, the engineer has to develop new techniques and processes that can be integrated with existing engine sub-systems to reduce pollutant output. The fuel injection equipment is one such sub-system that has been found to lend itself to development leading to improvement in engine performance and emission quality. These benefits have been achieved by increased controllability of the fuel injection process and the use of higher injection pressures. Ultimately the combustion process is determined by the quality of the fuel spray and its distribution and mixing within the combustion chamber. Break-up and distribution of the spray is largely determined by the in-cylinder conditions (air motion, density and temperature), the injection pressure, nozzle design and geometry.

The spray penetration length and spray penetration rate from a fuel injector are parameters used to judge fuel spray performance. The merits of high or low penetration largely depend on engine design and geometry. Shorter spray penetration may be of an advantage where it reduces fuel impingement, but in larger engines may inhibit maximum air utilisation [1]. Many correlations for fuel spray penetration have been proposed in the literature, a review of early correlations by Hay and Jones [2] has shown that there was disagreement in the results from the proposed correlations, although most investigators agreed that penetration was dependent on ambient density and injection pressure. Many of the initial investigations of spray performance were focused on low-pressure sprays injected into ambient or low density conditions [3]. More recent investigations by Hiroyasu and Arai [4], Naber and Siebers [5] have shown a strong dependency of spray penetration upon both in-cylinder pressure and fuel injection pressure. Hiroyasu and Arai [4] undertook comprehensive testing of the penetration and dispersion of both evaporating and non-evaporating sprays, and showed that the spray behaviour is strongly dependant on in-cylinder density. It was also concluded that in a higher density environment, wider dispersion of the spray occurred with increased amounts of air entrainment. This entrainment had a direct effect upon the momentum of the spray and hence reduced the penetration rate of the spray.

The study of Hiroyasu and Arai [4] also concluded that the in-cylinder temperature had a significant effect on spray penetration, reducing the penetration by as much as 20% compared to sprays injected into non-evaporating conditions. Similar effects of vaporisation were reported in the author's previous work (Morgan et al. [6]). Dent [7] suggested the inclusion of a term to compensate for these temperature effects:

$$S \propto \left(\frac{294}{T_a} \right)^{0.25}$$

However the observations of [5, 6] showed that this term does not fully compensate for the temperature effect on the liquid phase penetration.

A similar dependency of the liquid spray penetration on air density and in-cylinder pressure was observed by both Hiroyasu & Arai [4] and Dent [7], who found the following correlation:

$$S \propto \left(\frac{P_f - P_a}{\rho_a} \right)^{0.25}$$

It is important to state that the above correlation was based on investigations using mechanical pump injection systems. Modern common rail fuel injection equipment were used in the investigations of Naber and Siebers [5] and Morgan et al. [6], while injecting into high-density environments. Their results showed that this correlation over predicts the liquid penetration length. Naber and Siebers [5] suggested the following modification to compensate for the spray penetration dependence on injection and in-cylinder conditions:

$$S \propto \frac{(P_f - P_a)^{0.25}}{(\rho_a)^{0.345}}$$

This correlation although in a better agreement with the experimental measurements of Morgan et al. [6], still exhibited an over prediction of liquid phase spray penetration. It was concluded that this might be a consequence of differences in both injection rate profiles and nozzle geometries between the two studies [6].

It is clear from the above that although the influence of injection parameters has been widely investigated, information on the effects of in-cylinder density and fuel rail pressure on spray and fuel vapour distribution are still not conclusive.

It is generally accepted that injection rate profile and injection nozzle geometry are known to have a major influence on both the penetration and distribution of the fuel spray within the cylinder [12]. A reduction in the nozzle orifice diameter has also been shown to have an effect on the emissions [9]. This was concluded to be caused by the decreased size of droplets produced by smaller diameter nozzles. These smaller droplets mix and evaporate faster leading to shorter ignition delays. The internal flow structures within the nozzle are also thought to affect the spray performance. Hence different spray structures may not be attributed to differences in nozzle diameter only, but also to the nozzle type. Investigations into these flow process have been undertaken in both large scale and full size nozzles [10, 11]. The effects of cavitation within the nozzle have been identified as a major influence on the subsequent liquid/droplet behaviour. The variation in the behaviour of various nozzle types and the influence of injection rate may go some way to explaining the apparent differences in the correlations for penetration with time and dispersion found in the literature. This again highlighted the strong dependence of the fuel spray behaviour on the nozzle geometry and hence the dangers of applying generic correlations derived from experiments based on a limited specific nozzle type.

The multi-hole injection investigations of Bae and Kang [12] found that there was little hole-to-hole variation when injecting diesel through a VCO nozzle; however, an orifice-to-orifice variation was observed in spray angle when a sac nozzle was investigated. The experimental approach of Bae and Kang [12] allowed all orifices to discharge in the measurement vessel. However in the investigations of Campanella et al. [13] where the discharge from all the non-measured orifices were captured, variations in the performance of each orifice of a five hole VCO nozzle was found. It was also noted that the alteration of the needle seat construction had a strong influence on nozzle performance. Bae and Kang used a double-guided needle in this work and commented that previous results using a single-guided needle showed variations in penetration and dispersion. It is unclear whether the needle in the experiments of Campanella et al. was single or double-guided.

From the above, many of the experiments investigating spray characteristics have been undertaken with specially manufactured nozzles to facilitate data gathering. This normally means that a special single orifice nozzle is used or that all but one orifice discharge is captured. Measurements are then concentrated on one particular hole. The validity of such an approach is often questioned, as the adoption of this practice may influence the behaviour of the injection process. The data available in the literature pertaining to the investigation of multiple orifices versus single orifice nozzles is sparse. In addition, the information available on the hole-to-hole variation of sprays from particular injectors is contradictory and often appears to be dependent on the particular experimental approach adopted [12, 13].

The fuel evaporation, penetration with time and dispersion is important to the combustion process as it provides the transport of the fuel vapour into the chamber. The mixture of air and fuel vapour to the required chemical ratio provides suitable conditions for autoignition. Using Rayleigh scattering Dec [14] measured the simultaneous development of the liquid and vapour phases of the fuel spray. In this work it was found that the vapour did not penetrate further than the liquid core until the maximum liquid penetration length was reached. After this period the vapour continued to penetrate into the chamber. The width of the vapour phase was observed to develop to twice that of the liquid at the location of maximum liquid core penetration. As yet the influence of the injector characteristics on the

vapour distribution process has not been fully investigated.

In summary, although the investigation concerning the liquid penetration from diesel sprays has been quite extensive, a reliable correlation for the prediction of penetration with time has still to be developed. It is the belief that the discrepancies in the models presented are caused by the difference in injection nozzle geometries. The ambiguity over the effect of nozzle types on liquid phase penetration also extends to the vapour phase propagation. It is therefore clear that the effect of nozzle type and in-cylinder conditions on the injection and mixing processes are not fully understood.

The current work gives details of experiments undertaken to quantify both the liquid and vapour distribution of a diesel fuel injected through modern common rail fuel injection system into realistic engine environments (high-temperature charge experiments) and into in-cylinder conditions at lower temperatures than expected in a working engine (low-temperature charge). The rationale for investigating the low temperature charge conditions was initially to look at the effects of temperature on the evaporative processes of the spray and for later use as validation for CFD models. Injection using a range of fuel rail pressures and a number of in-cylinder density conditions are presented. The results are compared with other experimental data and empirical models. The effects of nozzle geometry are also discussed together with the validity of using specially manufactured nozzle types in these kinds of fundamental tests.

EXPERIMENTAL APPARATUS

Spray rig

A high-pressure spray rig was installed at the University of Brighton in 1999. This facility allows the testing of a wide range of injectors at different fuelling rates and pressures. The spray is injected into a rapid compression machine with a large optical chamber. In-cylinder pressures and temperatures up to 12 MPa and 750 K respectively can be achieved, by preconditioning the boost air supply. The optical chamber gives good visual access to the full spray. The design of this facility has been described in the past [15, 16]. The window dimensions were 53 mm in the vertical plane direction, by 23 mm in the horizontal plane.

A second generation Bosch common rail system [17] was used for this work, with a maximum rail pressure capability of 160 MPa. The fuel pump was powered by an electric motor running at 1400 rev/min ensuring a stable rail pressure with minimal fluctuation. The rail and delivery pipe were both instrumented with a 4067 Kistler pressure transducer. The pipe from the rail to the injector was kept short, representative of a passenger car. A custom controller was developed and is described in detail in [15]. This enabled independent control of injection timing, injection duration and rail pressure. The custom controller allowed control of initial needle drive current and PID control of the fuel rail pressure. The custom controller has built in time trigger outputs to allow the synchronisation of external equipment (cameras etc.) with the fuel injection process. A number of nozzles were used in this study, as described in Table 1.

Type	Orifice diameter [mm]	l/d	Number of orifices
VCO & Mini-sac	0.10	10.0	Single
VCO & Mini-sac	0.15	6.8	Single and five hole (VCO)
VCO & Mini-sac	0.20	5.0	Single, three and five hole (VCO)

Table 1. Nozzle details

The single-hole nozzle design had an equivalent cone angle of 130° . All injector holes were manufactured by conventional spark erosion technique and then micro-honed to produce an entry radius and surface finish representative of a production nozzle. The needle was of the single-guided type and was instrumented with a Hall effect type needle lift sensor. Fuel rail pressure and needle lifts were monitored on a digital storage oscilloscope. The nozzles and controller were calibrated on a Moewald test bed to establish the injection times required for different fuellings required by the experiments. Nozzle delivery rates were measured using a Lucas rate gauge. Nozzles were calibrated periodically during the test programme.

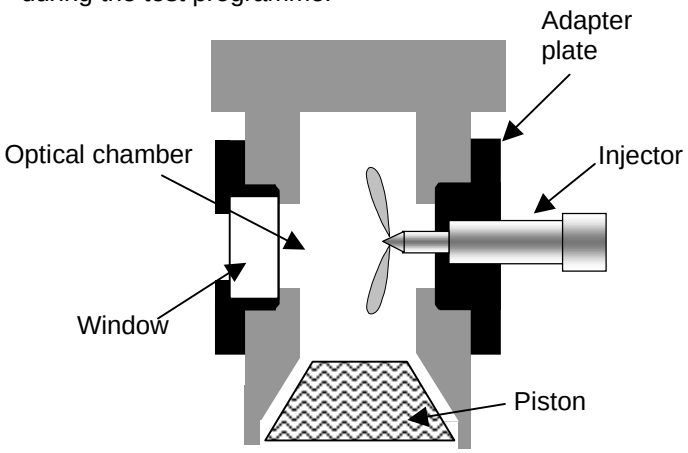

Figure 1. Injector adapter.

Modifications to the existing rig were made to facilitate the observation of multi-hole injector nozzles (Figure 1). This was done so that the differences in the performance of single vs. multi-hole and multi-hole (VCO) vs. multi-hole (sac type) nozzles can be visualised. The injector was orientated such that the spray of interest was vertical.

Image acquisition

Illumination of the spray was provided by halogen photo lamps as shown in Figure 2. Images of the spray produced from the range of nozzles tested were

captured on a Kodak Ektapro high-speed image Analyser (Model 4540). Recording rates were adjustable from 30 to 4500 frames per second at full resolution (256 ×256 pixels × 256 grey levels), and from 9000 to 40500 frames per second at progressively reduced resolution. The best compromise between acquisition rate and image resolution was obtained with a frame rate of 27000 pictures per second, with a corresponding resolution of 128×64 pixels. The camera was triggered off the injection pulse.

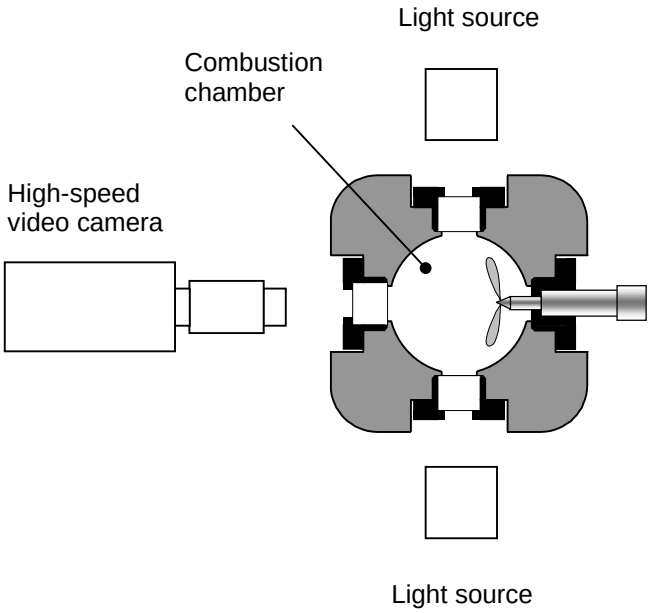

Figure 2. Injector adaptor plan view.

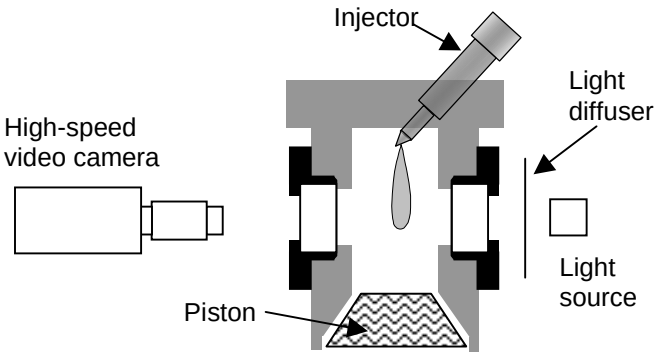

Figure 3. Representation of the setup for high-speed video recording of backlit spray.

To enable a full view of the development of a single spray, the setup described in Figure 3 was used. The sprays were backlit by a halogen photoflood fitted with a diffuser. Again the images were captured on an Ektapro Motion Analyser.

The high-speed video camera was set to a recording rate of 27,000 frames per second, allowing the entire injection phase to be recorded. The exposure of each frame was 37 µs and the uncertainty due to spray development during the exposure was measured to be ± 1 mm during the early stages of injection. This level of accuracy was derived from comparison with both spark-lit high-resolution photographs and laser-illuminated spray videos. The processing of the videos was performed by purpose-developed software that measures the spray penetration length and spray cone angle at each video frame after suitable pixel thresholding [6]. Repeatability tests were performed to assess the variability in penetration for a range of test conditions. The variation in penetration length was found to be ± 4% from the average curve. The camera resolution was measured to be 0.3 mm per pixel, hence the overall uncertainty was estimated to be ± 6%.

For vapour imaging a standard schlieren set-up was used as shown in Figure 4. The position of the injector for the Schlieren work was the same as for the full field spray work, as described in Figure 3. The schlieren images were directly recorded with a high-speed CCD video camera in order to optimise the quality of the video recordings.

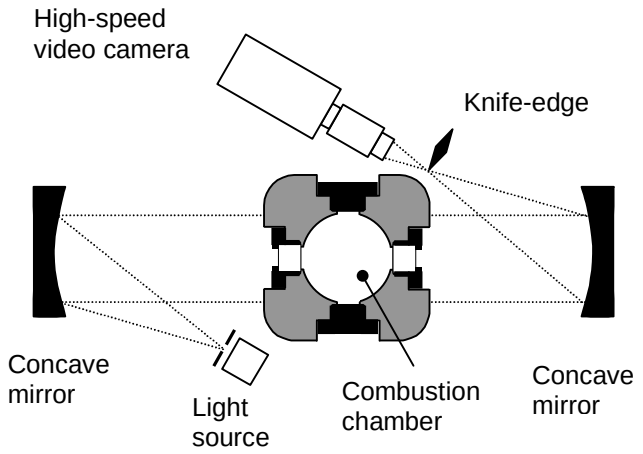

Figure 4. Set-up for high-speed video schlieren imaging.

A sodium light source was used with a variable iris, the light was reflected between two concave mirrors of 1.2 m focal length and diameter 144 mm. The light was brought to focus on the high-speed video camera, and the contrast of the image was controlled by an adjustable knife-edge. High-speed engine data were captured on a digital storage scope and a Ricardo Configurable High-speed Acquisition System for Engines (CHASE). Low speed data were recorded on the rig's logging computer. In-cylinder pressure traces were used to determine the conditions at injection for each experiment. The high-speed data were also used to calculate the density and temperature in the chamber at the time of injection. The processing of the videos was performed using thresholding in a similar way to the liquid phase imaging.

Experimental test conditions.

Over 600 test points were considered representing a comprehensive set of conditions. These conditions included a wide range of in-cylinder parameters, injection quantities and pressures, and a number of injector nozzle types that are typical of modern and futuristic diesel engine configurations. Table 2 lists the

conditions and experimental parameters. The results presented in this paper have been derived from data analysed from these test points. For brevity and clarity the figures presented are limited to few examples taken from this data set. The in-cylinder peak charge temperatures in table 2 have been calculated from data acquired during the experimentation. Charge temperature peaks at top dead centre and is reduced on the expansion stroke. For the low injection pressures (60 MPa) and a 30mm^3 fuelling (12° of crank) injected into a high-temperature charge with density 42 Kg/m^3 the in-cylinder charge temperature is estimated to drop by a calculated 37 K over the injection period.

Nozzle studies/Liquid penetration	
Nozzle types	VCO, Mini-Sac
Number of holes	Single, five and three
Hole diameters (mm)	0.1, 0.15, 0.2
In-cylinder densities (kg.m^{-3})	10 - 50
In-cylinder temperatures (K)	Low temperature 550 High temperature 700
Injection quantities (mm^3)	10, 30, 50
Injection pressure (MPa)	60, 100, 140, 160
Injection pulse width for 30 mm^3 0.2 VCO (ms)	4.2, 3.1, 2.6, 2.4
Schlieren Studies	
Nozzle types	VCO
Number of holes	Single
Hole diameters (mm)	0.2
In-cylinder densities (kg.m^{-3})	10 – 50
Injection quantities (mm^3)	30
Injection pressure (MPa)	60, 100, 140, 160
In-cylinder temperatures (K)	High temperature 700

Table 2. Experimental conditions. The fuel used was pump grade low sulphur diesel with a density of 840 kg/m^3. The fuel was held at 20° C (+ 5° C), returned fuel being cooled by a heat exchanger.

RESULTS AND DISCUSSIONS

The results from the nozzle close-up investigations were captured with the Motion Analyser. The video frames were downloaded on a PC for post-processing. These frames were combined to make a number of movies so that nozzle behaviour could be compared under identical injection and in-cylinder conditions. The outcome of these comparative studies is detailed below:

CLOSE-UP NOZZLE STUDIES

Many of the tests described and analysed within the paper were evaluated using single-hole nozzles. In the case of the single-hole VCO nozzles, an initial 'hesitation' period of flow was observed at the beginning of the visible injection (Figure 5). Figure 6 illustrates a comparison between a 0.2 mm single-hole nozzle and a 0.15 mm single-hole nozzle, along with a five-hole 0.15 mm nozzle. At about 0.148 ms after the spray became first visible, the 0.2 mm single-hole injector orifice seemed to shut very shortly before the needle reaches full lift. The same effect was visible to a lesser extent with the 0.15 mm single-hole nozzle at 0.185 ms. No such behaviour was observed with the multi-hole VCO or any of the sac type nozzles tested.

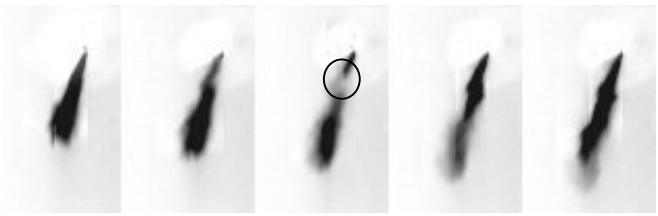

Figure 5. Hesitation at the opening phase of the VCO nozzle. Example shown is of a 10 mm^3 quantity of fuel injected at 160 MPa into a peak chamber pressure of 8 MPa. The nozzle is a 0.2 VCO.

In the needle lift traces the needle continues to lift during this period, this leads to the conclusion that the needle shuts the orifice by moving transversally rather than vertically. This pulsed closure of the orifice is believed to be due to temporary unbalanced pressures at the needle tip. Prior to lifting, pressures at the tip of the needle are balanced, but when the needle starts to lift the single-hole is uncovered and therefore a pressure differential is produced across the needle. This pressure differential gives rise to a resultant force, which causes the needle to move, covering the hole again for a short period. This effect was not observed with multi-hole nozzles. Since the holes are uniformly spaced-out around the nozzle, pressure is equal around the needle. Single-hole mini-sac nozzles do not exhibit this behaviour, as the needle does not cover the orifice directly.

Figure 7 graphically represents the liquid spray tip penetration and demonstrates the early hesitation in the opening phase of the single hole nozzle. Similar data were observed for the penetration profiles of each individual hole of a three-hole nozzle as shown in Figure 7. As can be clearly seen the effect of the hesitation in opening was to delay the spray penetration with time. However, the curve for the three-hole nozzle was offset to allow direct comparison of the penetration rates. The penetration rate from each hole was the same for the single and multi-hole nozzles once the nozzle was fully open. The same was true when comparing the five-hole and single-hole VCO nozzles.

This data set shows that care should be taken when comparing experimental results from a single hole nozzle with theoretical data. With the present approach an account can be taken of the offset caused by needle oscillations.

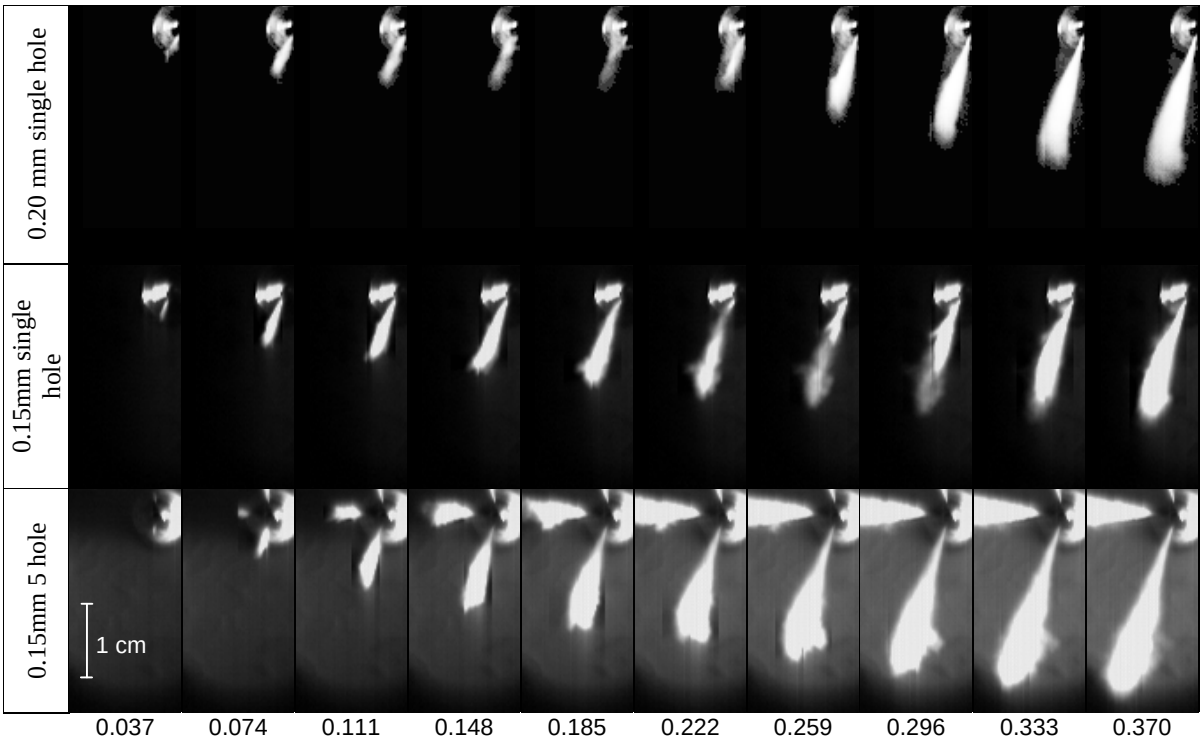

Figure 6. Comparison between 0.2 mm single-hole, 0.15 mm single-hole and 0.15 mm multi-hole nozzles. Injection pressure: 160 MPa and the fuelling was 10 mm^3 per nozzle orifice. Recording times are in milliseconds after first frame showing visible liquid injection.

Comparisons of double guided single-hole VCO nozzles and multi-hole VCO nozzles are planned in order to investigate this phenomenon further. Analysis of the video images revealed that both mini-sac and VCO nozzles started injecting at the same time after the trigger signal. A liquid spray was seen to exit the injector at the same frame number in each case approximately 0.44 ms after the injection signal. The needle lift traces of both types of nozzle confirm that start of needle lift occurs at the same time, approximately 0.23 ms after start of the injection signal, with full lift achieved by 0.86.

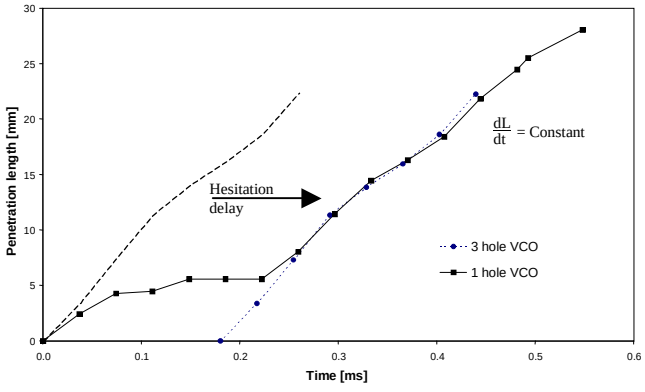

Figure 7. Single and multi-hole 0.2 mm VCO penetrations with time. 10 mm^3 fuelling per hole 160 MPa injection pressure ambient density 40 $kg.m^{-3}$.

Comparing the video data to the needle lift trace (Figure 8) it is clear that the spray became visible at the point when the needle began to accelerate rapidly (0.44 ms), rather than when it began to move. This behaviour was repeatable for all the tests carried out, including tests on the multi-hole nozzles. The delay response may be attributed to the finite time required for fuel to the space evacuated be the needle. After the apparent closing of the nozzle a small wisp of spray was seen to leave the nozzle. This phenomenon only occurred for some of the single-hole VCO nozzle closures. This may again be attributed to needle instability during the closure phase. The period of this second nozzle opening was approximately two frames (74 μs). In all cases, the actual visible spray for the VCO was 5 frames longer than the equivalent mini-sac nozzle, this related to the longer fuelling period required for an equivalent mass to be injected.

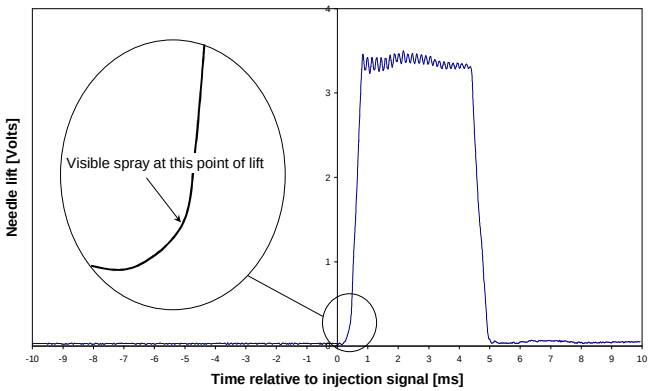

Figure 8. Injection needle lift trace (0.2 VCO nozzle, single hole 160MPa injection pressure).

The penetration with time for each of the holes of the multi-hole nozzles tested was evaluated in order to examine hole-to-hole variation. Comparative analysis of the liquid spray propagation for these measurements was limited to the first 22 mm of injection, the period when all sprays were contained within the viewing window. Many injection cycles and conditions were analysed frame by frame in a video-processing package in order to assess the radial propagation of the spray from each orifice. Analysis of the data showed that penetration profiles from each hole of the nozzles were approximately the same (Figure 9). A slight discrepancy in the magnitude of the penetration of each spray plume was observed, but these may be attributed to lighting. The multi-hole injector spray penetration characteristics (i.e. length and rate) were found to match those of the single-hole VCO (adjusted for needle hesitation, Figure 7) and single-hole mini-sac nozzles. It is therefore considered valid to use single-hole nozzles to characterise spray penetration, as long as the limitations mentioned above are taken into account. Further investigation with a more extensive range of nozzles is planned to determine whether this behaviour is the general case.

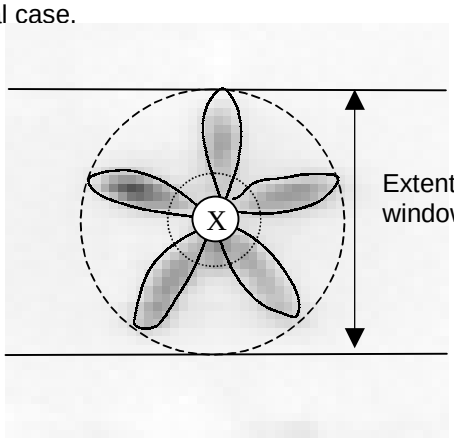

Figure 9. Spray penetration from a five-hole VCO nozzle. The centre of the injector is marked with an X. Lines are drawn to highlight the positions of spray plumes. The image was obtained with the method outlined in Figure 2.

FAR FIELD SPRAY STUDIES

Recordings were performed at three different injection pressures (60, 100 and 160 MPa), two intake air temperatures (20° C and 100° C), and several in-cylinder densities (14, 28, 34, 42, and 49 kg.m^{-3} at 20° C air intake; 14, 28, 35 and 40 kg.m^{-3} at 100° C). The majority of the tests were performed with a single-hole 0.2 mm VCO nozzle, with additional experiments performed on 0.2 mini-sac and 0.15 mm VCO nozzles for comparison purposes.

Low temperature charge

After the initial hesitation the liquid penetration profiles for low-temperature charge clearly show two distinct phases: an almost linear increase in penetration lasting between 1 ms (160 MPa injection) and 1.5 ms (60 MPa) with a rapid transition to a steadier penetration length. During the latter phase, the penetration profiles fluctuate around a slowly increasing average. These fluctuations were found to be slugs of fuel breaking away from the main liquid core. One has to bear in mind that these tests were performed under non-firing conditions, and therefore any data gathered after the theoretical firing time may be directly relevant to real engine conditions. However it offers an improved understanding of spray formation.

The effect of gas density on spray penetration profiles was found to follow the trends observed by Naber and Siebers [5], although a comprehensive comparison cannot be made at this stage because of the more focused density range used here (14 to 49 kg.m^{-3}, as opposed to 3.6 to 124 kg.m^{-3} in [5]).

At in-cylinder densities between 28 and 49 kg.m^{-3}, the ultimate spray penetration length varied between 50 and 60 mm, and was directly dependant on ambient density and injection pressure.

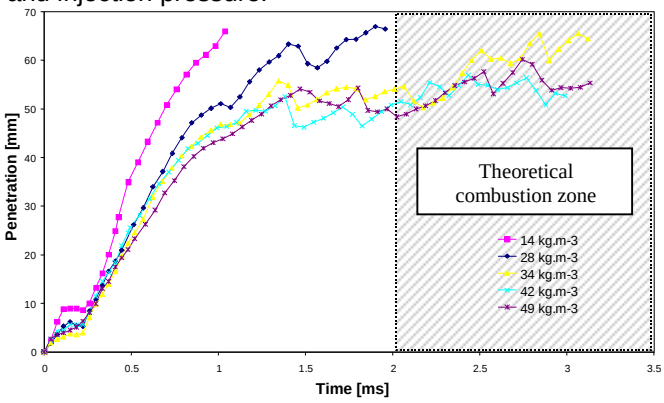

Figure 10. Influence of ambient density on penetration for low-temperature charge. Injection pressure: 160 MPa, 0.2 VCO single hole nozzle with a 30mm^3 fuelling.

The injection pressure was found to have a significant effect on the rate of penetration of the liquid core as can be seen in Figure 11. As expected higher injection pressures produce fully developed sprays in a shorter time, thus improving the vaporization process as the surface area of the liquid core increases.

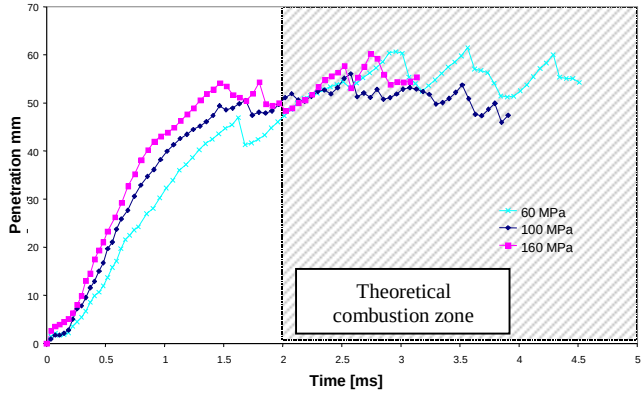

Figure 11. Influence of injection pressure on penetration for low-temperature charge. 49 kg.m^{-3} in-cylinder density

0.2 mm VCO Nozzle. Shaded area shows region with high-probability of ignition.

Sprays injected into the 34Kg/m^3 in cylinder density at different injection pressures showed similar dispersion trends. After an initial wide spray cone, the cone angle steadily reduced reaching a stable dispersion full cone angle of 11° (Figure 12). No noticeable relationship between the injection pressure and the spray dispersion angle were found.

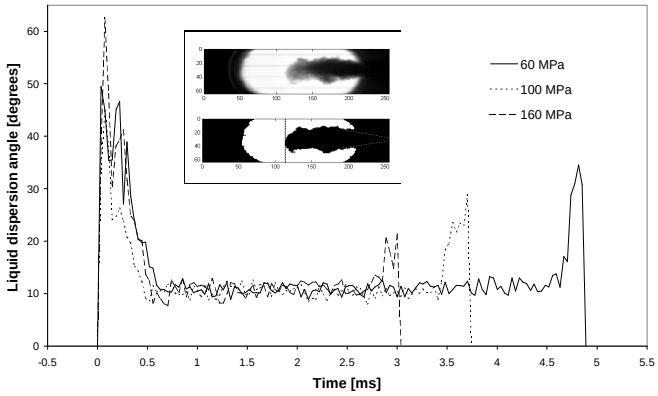

Figure 12. Evolution of spray full cone angle at different injection pressures. Low temperature charge, in-cylinder density: 34 kg.m^{-3} and a 0.2 mm single hole VCO nozzle.

The spray penetration profile data were compared with the correlations proposed by Hiroyasu and Arai [4]. Unlike the sprays of Hiroyasu and Arai, in the current tests, the spray break-up was observed to be almost instantaneous. The linear correlation of [4] for the break-up period was therefore not applicable in this case. Figure 13 illustrates the application of their logarithmic correlation used for the post break-up period described in the following relation:

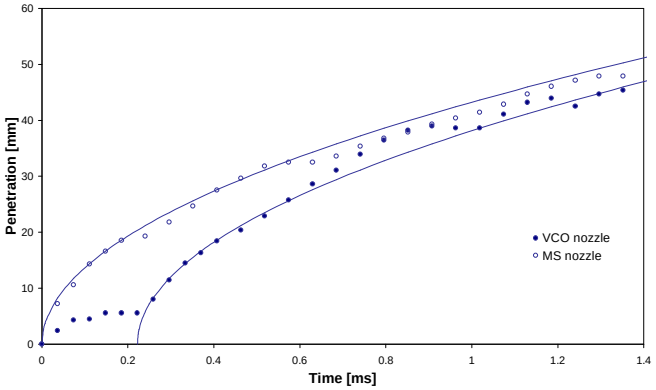

Figure 13. Comparison between mini-sac and VCO single-hole nozzles and the correlation proposed by Hiroyasu and Arai [4] for non-evaporating sprays. Injection pressure: 160 MPa. In-cylinder density: 42 kg.m^{-3}.

$$S = K\left(\frac{P_{inj} - P_a}{\rho_a}\right)^{0.25}\sqrt{D.t} + C$$

Where S is the spray penetration, K is an empirical constant, P_{inj} the injection pressure, P_a the ambient pressure, ρ_a the ambient density, D the injector orifice diameter, t is the time after start of injection and C is a correction time constant.

A coefficient (K) of 6.5 instead of 2.95 [4] was found to give best agreement with the experimental data, both for mini-sac and VCO type nozzles. For the single-hole VCO nozzles, the initial injection hesitation period was taken into account by the addition of a time constant (C).

High-temperature charge

The liquid penetration profiles are similar in shape as for the low-temperature charge tests, except that the liquid sprays were still viewable through the window at the lowest ambient density. The profiles also show a similar rapid penetration followed by fluctuations around a slowly increasing average penetration length. As opposed to the low-temperature charge tests, the ambient density has a noticeable effect on the ultimate penetration length: the higher the density, the shorter the liquid penetration (from about 55 mm at 14 kg.m^{-3} to 30 mm at 40 kg.m^{-3}). In addition the injection pressure and ambient density were also found to have a greater influence on the initial increase in penetration with time. As for the low temperature conditions it was found that higher injection pressures increased the penetration rate due to the greater liquid momentum.

As for the sprays injected into low-temperature charge, a wide spray cone angle was found at the very beginning of the injections, progressively reducing to a narrower mean spray full cone angle of 10°. Lower injection pressures resulted in an increased average spray dispersion angle. Further tests are planned to for a more in depth analysis.

It was found that early liquid core propagation velocities, calculated for the early linear part of the injections (after the hesitation period between 0.3 and 0.8ms in Figure 11), seem to decrease linearly with increasing gas densities. The tests were performed at three different injection pressures (60 MPa, 100 MPa and 160 MPa) and at two intake conditions (cold and pre-heated). For the cold intake air, these initial liquid velocities are grouped in the low-density/high-velocity area, then diverging from each other as density increases (Figure 14). The spray injected at the higher pressure exhibited lower decrease in velocity over the in-cylinder density range tested. Opposite trends were found when the intake air was heated as can be seen from Figure 15. The velocity profiles converged as the gas density increased to reach the same velocity (about 23 m.s^{-1}). The largest velocity drop was obtained at the highest injection pressure.

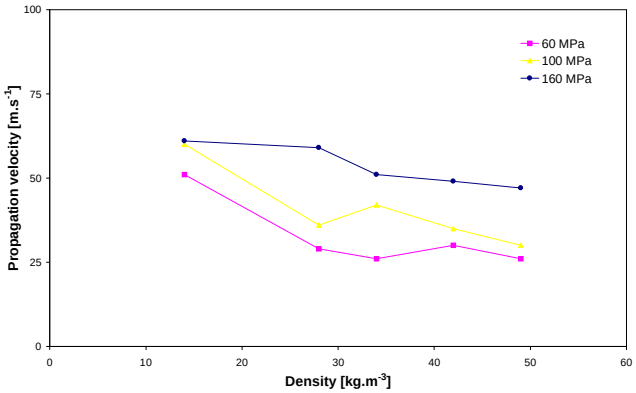

Figure 14. Influence of in-cylinder density on spray propagation velocity at different injection pressures. Low-temperature charge.

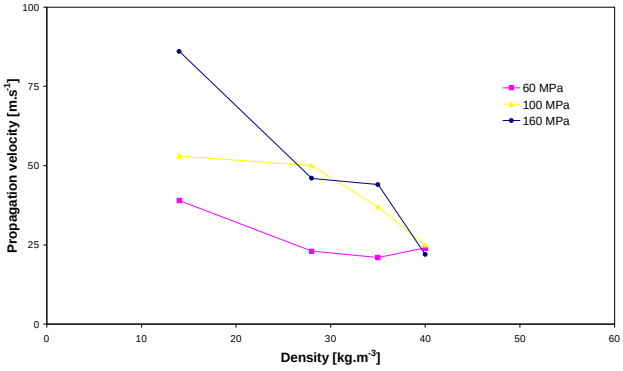

Figure 15. Influence of in-cylinder density on spray propagation velocity at different injection pressures. High-temperature charge.

Vapour dispersion imaging

The vapour penetration was analysed using schlieren video. Similar penetration with time were observed in all the test cases. The following trends were observed in the imaging videos at all test conditions. The vapour developed alongside the liquid core during the early stages of injection with the width of the vapour cloud becoming wider as the liquid penetrated into the chamber. This was believed to be a consequence of the combination of local turbulent mixing and the gradual increase in vapour concentration. When the liquid core reached its ultimate stable length (Figure 16, Figure 17), the vapour continued to penetrate into the chamber at a similar rate to the liquid spray injected into an equivalent ambient density of lower charge temperature. The vapour cloud increased in width as it penetrated, ultimately occupying the width of the visible chamber, becoming obscured by the window holders.

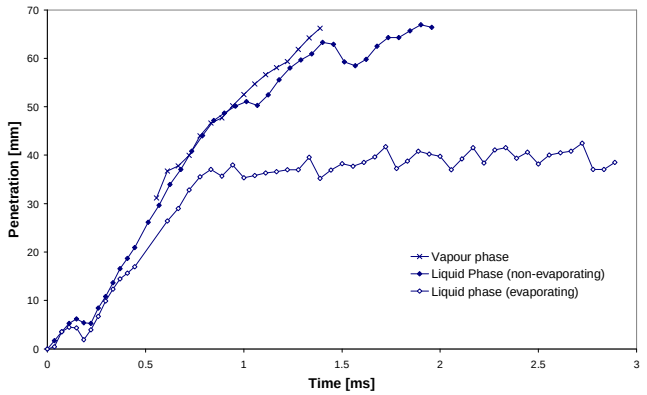

Figure 16. Vapour and liquid penetrations for both temperature charge conditions. 160 MPa injection pressure; 28 kg.m^{-3} in-cylinder density.

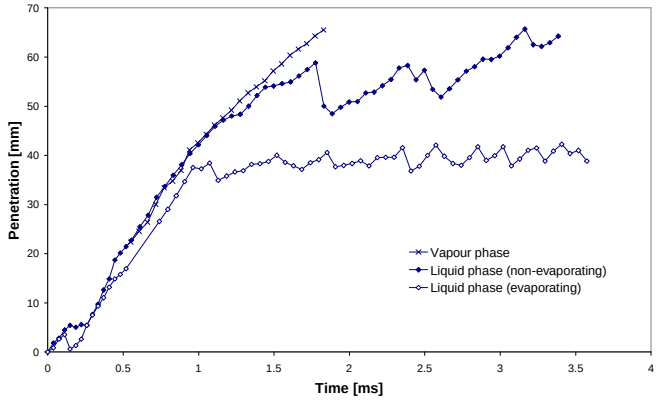

Figure 17. Vapour and liquid penetrations for both temperature charge conditions. 100 MPa injection pressure; 28 kg.m^{-3} in-cylinder density.

Tests were performed to determine the repeatability of the results obtained from the schlieren experiments (Figure 18). The same test was conducted four times. The maximum deviation of any profile from the average was below 8.3%.

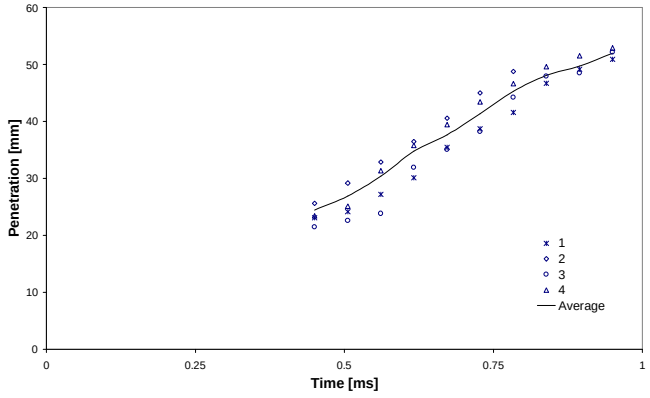

Figure 18. Schlieren repeatability tests. Injection pressure: 140 MPa. In-cylinder density: 22 kg.m^{-3}.

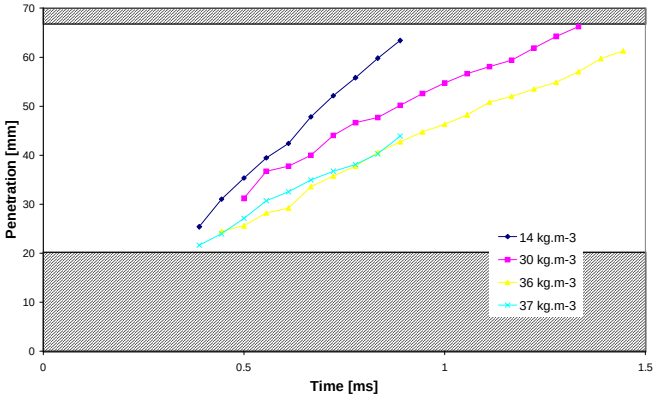

Figure 19. Influence of gas density on vapour penetration.160MPa injection pressure 0.2 VCO nozzle. Hatched area is outside of rig optical access.

The vapour penetration had a linear relationship with time for all conditions tested (Figure 19). The profiles for both charge-temperature conditions slowly diverge after 0.5 ms from the start of injection. The rate of diversion depended upon the ambient density and injection pressure. Not surprisingly, the highest rate of vapour propagation was found to occur with the highest injection pressures into the lowest densities. It was observed that higher injection pressures seemed to promote faster vapour propagation at the very early stage of the injection, but the data gathered at this stage is not comprehensive enough to allow definite conclusions to be made (Figure 20).

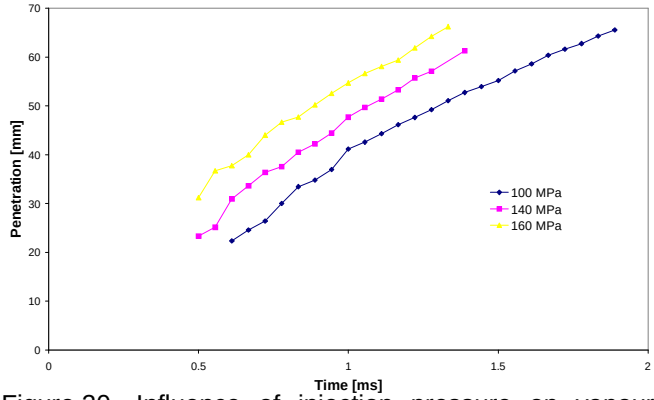

Figure 20. Influence of injection pressure on vapour penetration. 30kg/m^3 charge density 0.2 VCO nozzle.

The findings of this work on vapour penetration with time agree with both that of Dec [14] and Naber and Siebers [5] where vapour was observed to linearly penetrate across the chamber with time. It is suggested that the mechanism for the vapour transport is the gas motion induced by the liquid phase exchanging momentum from the droplets to the gas phase. Increased penetration of the vapour was observed at higher injection pressures and lower gas densities, i.e. when the liquid phase has a higher momentum. Rhim and Farrell [18] found that a multi-hole injector developed a different gas flow field than a single-hole nozzle as a result of the interaction in the flow between each spray plume. Hence if the air motion generated by the spray is the carrier of the vapour phase, then care must be taken in applying vapour penetration results from single-hole to multi-hole scenarios.

CONCLUSIONS

Through the acquisition of high temporal resolution images, the influence of the injector nozzle type on the formation, break-up and evaporation of a diesel spray was studied. This investigation found the following:

- The liquid phase penetration results from a previously unused multi-hole diesel nozzle from a modern common rail system suggested that, a liquid jet with comparable temporal penetration was produced by each orifice during the early stages of injection. This was found to be true over a range of injection pressures, fuelling quantities and in-cylinder conditions.

- Pressure fluctuations in the injector nozzle and hence needle deflection resulted in a different early stage injection behaviour for the single-hole VCO nozzle when compared to its multi-hole counterpart. Although this resulted in the addition of a predictable delay at the beginning of the liquid penetration process the subsequent liquid penetration rate was unaffected. The delay was due to a momentary closure of the orifice by the needle.

- It is therefore valid to use a single-hole VCO nozzle and derive effects for the multi-hole if this initial delay is taken into account.

- This trend was not observed for the single-hole mini-sac nozzles, where fluctuation of the needle would not cause premature orifice closure.

- The liquid core penetration profile for different nozzles was dependent upon the injection pressure and in-cylinder conditions, with similar trends to those reported in previous work [4, 5].

- A new coefficient for the empirical model of Hiroyasu and Arai [4] were derived from the experimental data. This coefficient was shown to be applicable for both the mini-sac and VCO nozzles. The VCO required an additional time offset constant to counteract the initial hesitation period.

- It was observed that the leading edge of the vapour phase penetrated at a similar rate to the liquid core until the liquid core had reached its ultimate length. After this time the vapour phase continued and penetrated deeper into the chamber due to earlier liquid/air momentum transfer.

- The vapour penetration profiles were shown to be dependent upon both injection pressure and in-cylinder density. An increase in injection pressure and decrease in in-cylinder density gave rise to

greater vapour penetration. These vapour results concur with the findings in the literature [5].

ACKNOWLEDGMENTS

We would like to acknowledge the EPSRC loan pool for providing access to equipment used in gathering the data presented. Special thanks to Valerie Pinault for her help in processing the data, and to Dave Jones and Paul Fryer of Ricardo Consulting Engineers for their assistance with the fuel injection equipment. Thanks also to Olivier Laguitton of Ricardo Consulting Engineers for his assistance in the final preparation of this paper.

REFERENCES

1. Bergstrand, P., and Denbratt, I., “Diesel Combustion with Reduced Nozzle Diameter”, SAE paper 2001-01-2010, 2001.
2. Hay, N., and Jones, J.L., “Comparison of the Various Correlations for Spray Penetrations”, SAE paper 720226. 1972.
3. Kuniyoshi, H., Tanabe, H., Sato, G.T. and Fujimoto, H., “Investigation on the Characteristics of Diesel Fuel Spray”, SAE paper SAE 800968, 1980.
4. Hiroyasu, H., and Arai, M. “Structure of Fuel Sprays in Diesel Engines”. Transactions of the SAE Vol 99, Sect 3, pp 1050-1061, 1990.
5. Naber, J., and Siebers, D.L., “Effects of Gas Density and Vaporization on Penetration and Dispersion of Diesel Sprays”. SAE 960034, 1996.
6. Morgan, R., Wray, J., Kennaird, D. A., Crua, C., Heikal, M., “The Influence of Injector Parameters on the Formation and Break Up of a Diesel Spray”. SAE 2001-01-0529, 2001.
7. Dent, J.C., “A Basic Comparisons of Various Experimental Methods for Studying Spray Penetration”. SAE 71057, 1971.
8. Schmidt, D.P., and Corradini, M.L., “The Internal Flow of Diesel Fuel Injector Nozzles: a Review”. International Journal of Engine Research, Vol 2 part 1, IMechE. 2001.
9. Bergstrand, P. and Denbratt, I., “Diesel Combustion with Reduced Nozzle Orifice Diameter”. SAE 2001-01-2010, 2001.
10. Badock, C., Wirth, R., Fath, A. and Leipertz A., “Investigation of Cavitation in Real Size Diesel Injection Nozzles”. International Journal of heat and Fluid Flow, Vol 20, 1999 pp534-544 .
11. Soteriou, C., Andrews, R., and Smith, M., “Direct Injection Diesel Sprays and the Effect of Cavitation and Hydraulic Flip on Atomization”. SAE 950080. 1995.
12. Bae, C. H. and Kang, J., “Diesel Spray Characteristics of Common-Rail VCO Nozzle Injector”, Thiesel 2000, Valencia 13-15 September 2000.
13. Campanella, R. Laforgia, D., Ficarell, A. and Damiani, V., “Spray Characteristics of Five-Hole V.C.O. Nozzles of a Diesel Electro-injector”. SAE 940192, 1994.
14. Dec, J. E., “A Conceptual Model of DI Diesel Combustion Based on Laser-Sheet Imaging”. SAE 970873, 1997.
15. Kennaird, D. A., Crua, C., Heikal, M., Morgan, R., Bar, F., Sapsford, S., “A New High Pressure Diesel Spray Research Facility”, Computational and Experimental Methods in Reciprocating Engines, I.Mech.E. Conference transactions, 1-2 November 2000.
16. Morgan, R.E., Kennaird, D.A., Heikal, M.R., and Bar, F., “Characterization of a High Pressure Diesel Fuel Spray at Elevated Pressures”. Thiesel 2000, Valencia 13-15 September 2000.
17. Stumpp, G., and Ricco, M., “Common Rail – An Attractive Fuel Injection System for Passenger Car and DI Diesel Engines”. SAE 960870. 1996
18. Rhim, D. and Farrell, P.V. Effect of Gas Density and the Number of Injector Holes on the Air Flow Surrounding Non-Evaporating Transient Diesel Sprays. SAE 2001-01-0532

CONTACT

Any correspondence should be addressed to Dr Dave Kennaird: D.A.Kennaird@brighton.ac.uk